

# Proposal and analysis of a silica fiber with large and thermodynamically stable second order nonlinearity

Yong Xu<sup>a)</sup> and Anbo Wang

Department of Electrical and Computer Engineering, Virginia Polytechnic Institute and State University, Blacksburg, Virginia 24061

James R. Heflin

Department of Physics, Virginia Polytechnic Institute and State University, Blacksburg, Virginia 24061

Zhiwen Liu

Department of Electrical Engineering, The Pennsylvania State University, University Park, Pennsylvania 16802

(Received 11 March 2007; accepted 23 April 2007; published online 23 May 2007)

The authors propose a general approach that can produce a silica fiber with large and thermodynamically stable second order nonlinearity. They estimate that it is possible to achieve second harmonic generation efficiency of more than 10% in such a nonlinear fiber with a length of a few hundred microns. By maintaining a high degree of spatial symmetry, the proposed nonlinear fiber can naturally generate polarization entangled photon pairs, a physical object of enormous significance for quantum information technology. © 2007 American Institute of Physics.

[DOI: 10.1063/1.2740472]

An important principle of nonlinear optics<sup>1</sup> is that second order nonlinearity is impossible for any centrosymmetric materials. This stringent requirement essentially excludes some of the most important materials, such as silica fibers, from the list of candidates that can be considered for second order nonlinearity. In this letter, we demonstrate that it is possible to generate very strong second order nonlinear responses in silica based fibers with full cylindrical symmetry. As shown in Fig. 1, the proposed nonlinear fiber possesses a cylindrical silica core and a layer of nonlinear molecules oriented along the radial direction. In the following analysis, we demonstrate that the proposed fiber in Fig. 1 can provide large and thermodynamically stable second order nonlinear responses. Furthermore, instead of being a hindrance, the full rotational symmetry of the nonlinear fiber can actually lead to conservation laws that can be used to generate polarization entangled photon pairs.

We begin our analysis by considering the case of sum frequency generation in the proposed fiber. To make our analysis as general as possible, we start from a single assumption: The nonlinear fiber is uniform along the direction of wave propagation (i.e., the  $z$  axis). In this case, the waveguide mode at frequency  $\omega_1$  can be expressed as<sup>2</sup>

$$\mathbf{E}_{\omega_1}(\mathbf{r}) = \text{Re}\{E_{\omega_1} \exp[i(\omega_1 t - \beta_1 z)] \mathbf{u}_{\omega_1}(\mathbf{r})\}. \quad (1)$$

In Eq. (1),  $E_{\omega_1}$ ,  $\beta_1$ , and  $\mathbf{u}_{\omega_1}(\mathbf{r})$  are, respectively, the field amplitude, propagation constant, and transverse field distribution at frequency  $\omega_1$ . For the other two frequency components of the nonlinear process, we similarly define  $E_{\omega_2}$ ,  $\beta_2$ , and  $\mathbf{u}_{\omega_2}(\mathbf{r})$ , and  $E_{\omega_3}$ ,  $\beta_3$ , and  $\mathbf{u}_{\omega_3}(\mathbf{r})$  at  $\omega_2$  and  $\omega_3$ , respectively. In sum frequency generation, two photons at frequencies  $\omega_1$  and  $\omega_2$  are converted into a sum frequency photon at  $\omega_3$ , with  $\omega_3 = \omega_1 + \omega_2$ . Following the procedures in Ref. 3, we find that the amplitude of the sum frequency mode is given by

$$\frac{dE_{\omega_3}}{dz} = -i \frac{\omega_3}{2\varepsilon_0 v_g} E_{\omega_1} E_{\omega_2} \times \exp(-i\Delta\beta z) \int \int_S \mathbf{u}_{\omega_3}^* \cdot \chi^{(2)} : \mathbf{u}_{\omega_1} \mathbf{u}_{\omega_2} ds, \quad (2)$$

where  $\chi^{(2)}$  is the second order nonlinear susceptibility tensor,  $v_g$  is group velocity at  $\omega_3$ ,  $\Delta\beta = \beta_{\omega_1} + \beta_{\omega_2} - \beta_{\omega_3}$  describes phase mismatch, and the integration is over the fiber cross section  $S$ . The full derivation of Eq. (2) will be published separately. Comparing Eq. (2) with the standard result for sum frequency generation,<sup>2</sup> we find that the two results are almost identical, as long as we use the following parameter  $D_{\text{eff}}$  as an effective nonlinear coefficient to describe the nonlinear process within the fiber:

$$D_{\text{eff}} = \int \int_S \mathbf{u}_{\omega_3}^* \cdot \chi^{(2)} : \mathbf{u}_{\omega_1} \mathbf{u}_{\omega_2} ds. \quad (3)$$

To further simplify the analysis, we assume that the  $\chi^{(2)}$  tensor is dominated by its radial components  $\chi_{rrr}^{(2)}$ . (This assump-

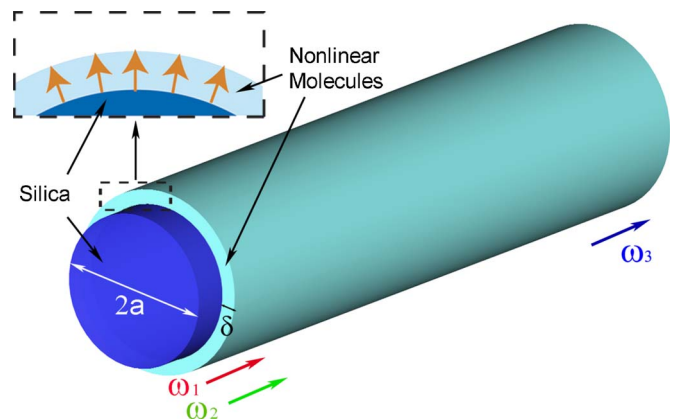


FIG. 1. (Color online) Schematic of the proposed nonlinear fiber with full cylindrical symmetry. The radially aligned nonlinear molecules provide a second order susceptibility tensor dominated by the  $\chi_{rrr}^{(2)}$  component.

<sup>a)</sup>Electronic mail: yong@vt.edu

tion is consistent with the nonlinear material we envision for use in experimental implementation of the proposed fiber.) In this case, we can express the effective nonlinear coefficient  $D_{\text{eff}}$  as

$$D_{\text{eff}} = \int_0^\infty r dr \int_0^{2\pi} d\theta [\chi_{rrr}^{(2)} u_{\omega_3,r}^* u_{\omega_1,r} u_{\omega_2,r}], \quad (4)$$

where  $u_{\omega_1,r}$ ,  $u_{\omega_2,r}$ , and  $u_{\omega_3,r}$  are the radial electric field components at  $\omega_1$ ,  $\omega_2$ , and  $\omega_3$ , respectively. Since the fiber is cylindrically symmetric, we can assign each fiber mode an angular modal number  $l$  and express its azimuthal dependence as  $\exp(il\theta)$ .<sup>2</sup> If we use  $l_1$ ,  $l_2$ , and  $l_3$  to denote the angular modal number of the modes at  $\omega_1$ ,  $\omega_2$ , and  $\omega_3$ , respectively, according to Eq. (4), we have

$$l_3 = l_1 + l_2 \quad \text{for any } |l_3\rangle \Leftrightarrow |l_1\rangle |l_2\rangle, \quad (5)$$

where we use  $|l_1\rangle$ ,  $|l_2\rangle$ , and  $|l_3\rangle$  to denote the polarization states of the photons at  $\omega_1$ ,  $\omega_2$ , and  $\omega_3$ , respectively. Equation (5) tells us that the total angular modal number must be conserved during any second order nonlinear process. This conservation law directly comes from the cylindrical symmetry of the nonlinear fiber, and its validity does not depend on the specific form of the  $\chi^{(2)}$  tensor, as can be seen from Eq. (3).

The conservation law in Eq. (5) can be used to generate polarization entangled photon pairs, a critical component in the emerging field of quantum information technology.<sup>4</sup> At the most basic level, this conservation law is very similar to the conservation of angular momentum in quantum physics. To illustrate this point, let us consider the process of spontaneous parametric downconversion (SPDC), widely used for the generation of polarization entangled photon pairs.<sup>5</sup> In SPDC, a higher frequency photon at  $\omega_p$  is spontaneously split into a signal photon at  $\omega_s$  and an idler photon at  $\omega_i$ . If the pump photon is in a TM mode (with  $l=0$ ), the two angular modal numbers of the signal photon and the idler photon must be equal in amplitude but opposite in sign. In other words, if the signal photon is in the state of  $|l\rangle$ , the idler photon must be in the state of  $|-l\rangle$ , and vice versa. Furthermore, due to the cylindrical symmetry of the nonlinear fiber, the probability of finding the signal photon in  $|l\rangle$  state or in  $|-l\rangle$  state must be equal. With these considerations, we conclude that the SPDC process in the nonlinear fiber can convert a pump photon in the state of  $|l=0\rangle$  into a signal and an idler photon in the state of  $[|l\rangle |-l\rangle + \exp(i\varphi) |-l\rangle |l\rangle] / \sqrt{2}$ , a polarization entangled state. This is exactly the optical equivalent of the famous EPR experiment, where a single spin 0 particle is split into two quantum entangled spin  $\frac{1}{2}$  particles.

From the discussion above, it is clear that the formation of quantum entanglement depends critically on the full cylindrical symmetry of the nonlinear fiber. A fully cylindrically symmetric configuration, however, is difficult to achieve using traditional means. The most common approach of generating second order nonlinearity in silica fiber is through optical,<sup>6</sup> electrical,<sup>7</sup> or UV poling.<sup>8</sup> All poling techniques, however, involve introducing a preferred direction in silica glass, therefore breaking the full cylindrical symmetry of the fiber. Furthermore, the poled fiber becomes thermodynamically unstable, which means that the induced second order nonlinearity can decay in a few months.<sup>9</sup> We also notice that it is very difficult to use nonlinear crystals such as LiNbO<sub>3</sub> to create the structure shown in Fig. 1.

Instead of the conventional approaches mentioned above, we can produce the proposed nonlinear fiber through polyelectrolyte multilayer self-assembly,<sup>10</sup> by coating a cylindrical silica fiber taper with nonlinear molecules, one layer at a time. A silica fiber taper with a micron scale radius can be realized through HF etching.<sup>11</sup> After producing the silica taper, the coating of the nonlinear molecules can be accomplished through a hybrid covalent/ionic self-assembly approach developed by one of the authors. Using this hybrid approach, a planar glass substrate coated with hundreds layers of nonlinear molecules such as Procion Brown MX-GRN has been experimentally fabricated.<sup>12</sup> Through second harmonic generation (SHG) measurements, the Procion Brown molecules were determined to be aligned predominately along the normal direction of the glass substrate ( $z$  axis). As a result, the nonlinearity of the Procion Brown film was found to be dominated by the  $zzz$  component, with  $\chi_{zzz}^{(2)} = 14$  pm/V, approximately half the value of LiNbO<sub>3</sub>.<sup>12</sup> The self-assembled films exhibit excellent temporal and thermal stabilities with no decrease of  $\chi_{zzz}^{(2)}$  after a temperature cycle to 150 °C for 24 h or under ambient conditions for more than two years.<sup>12</sup> They are also mechanically stable and impervious to immersion in water or most organic solvents. We can directly apply this hybrid self-assembly approach and coat a tapered cylindrical silica fiber with nonlinear molecules, therefore producing the proposed nonlinear fiber illustrated in Fig. 1. The thickness of a single layer of nonlinear molecules is typically in the range of 1 nm, and is significantly smaller than the radius of the tapered fiber. Therefore, the nonlinear molecules should still align predominately along the normal direction of the silica surface and provide a large  $\chi_{rrr}^{(2)}$  component. We also point out that the radial alignment of the nonlinear molecules is determined by electrostatic interaction, and is the thermodynamical ground state. As a result, the proposed nonlinear fiber should possess a second order nonlinearity that is thermodynamically stable, which is a significant advantage over the conventional poling techniques.

Besides demonstrating symmetry enforced quantum entanglement, the proposed nonlinear fiber is also highly efficient in terms of generating nonlinear photons. We can use SHG as a benchmark to characterize the efficiency of second order nonlinear processes in the proposed fiber. From Eq. (2), the SHG efficiency  $\eta_{\text{SHG}}$ , defined as the ratio of the optical power at the second harmonic ( $P_{2\omega}$ ) and at the fundamental frequency ( $P_\omega$ ), can be estimated as

$$\eta_{\text{SHG}} = \frac{P_{2\omega}}{P_\omega} \approx 2\omega^2 \left( \frac{\mu_0}{\epsilon_r \epsilon_0} \right)^{3/2} \frac{P_\omega}{\pi a^2} \left| \frac{\delta}{a} \chi_{rrr}^{(2)} \right|^2 L^2. \quad (6)$$

In deriving Eq. (6), we assume the following. (1) Phase matching is satisfied (this can be accomplished through modal dispersion matching,<sup>13</sup> by controlling the dimension and the index profile of the nonlinear fiber); (2) the polarization selection rule, i.e., Eq. (5), is satisfied; (3) the nonlinear fiber possesses a length of  $L$  and an effective modal area of  $\pi a^2$ ; (4) undepleted pump; (5) the loss in the nonlinear material can be neglected; (6) the nonlinear coating possesses a thickness of  $\delta$  and its  $\chi^{(2)}$  tensor is dominated by the  $\chi_{rrr}^{(2)}$  component; (7) the optical field intensity within the nonlinear coating can be approximated by the average field intensity within the silica core. The assumption (7) is valid for nonlinear fibers with micron scale silica cores. In Fig. 2, we

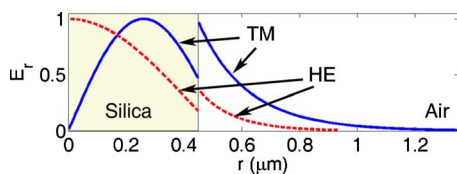


FIG. 2. (Color online)  $E_r$  field distribution of the fundamental HE and TM modes (at  $\lambda=775$  nm) in a cylindrical fiber with a silica core ( $0.9 \mu\text{m}$  in diameter) and an air cladding.

show the distributions of the radial component of the electric field for the fundamental HE mode and TM mode, respectively. The fiber is assumed to be a cylindrical step index fiber with a silica core of  $0.9 \mu\text{m}$  in diameter and an air cladding. The presence of the nonlinear layer, whose thickness is in the range of tens of nanometers, can be ignored in the calculation of electric field. For both the HE mode and the TM mode, the strength of  $E_r$  component at the air-silica interface, which corresponds to the value within the nonlinear layer, is clearly of the same order of magnitude as the average field strength within the silica core. We also observe that due to the large silica-air index contrast, both the HE mode and the TM mode are well confined within the silica core.

Comparing Eq. (6) with standard results for SHG efficiency,<sup>2</sup> we find that the two results are exactly the same, as long as we (1) replace the beam spot in a bulk nonlinear crystal  $A$  by the effective fiber modal area  $\pi a^2$ ; and (2) replace the bulk nonlinearity  $\chi^{(2)}$  by the effective nonlinearity  $(\delta/a)\chi^{(2)}$ . According to Eq. (6), by using a nonlinear fiber with a very small modal area, it is possible to enhance the efficiency of any second order nonlinear processes by several orders of magnitude. The appearance of the geometrical factor  $(\delta/a)$  is far from unique: it essentially plays the same role as the confinement factor  $\Gamma$  in the analysis of optical gain in quantum well lasers.

Using Eq. (6), we can easily estimate the SHG efficiency in a nonlinear fiber. For the nonlinear layer, we assume its thickness  $\delta$  is 50 nm and  $\chi_{rrr}^{(2)}$  value half of  $\text{LiNbO}_3$ . We assume a fiber radius of  $1 \mu\text{m}$ , which gives us an effective

$\chi^{(2)}$  approximately 2.5% of bulk  $\text{LiNbO}_3$ . We assume a pump wavelength of  $1 \mu\text{m}$  and a peak power of 100 kW (readily available from nanosecond and picosecond lasers). Using these values, Eq. (6) tells us that SHG efficiency can reach the level above 10% with a fiber length of  $200 \mu\text{m}$ . This remarkable result means that we do not even need a long nonlinear fiber to demonstrate highly efficient second order nonlinear processes. A nonlinear fiber of a few hundred microns in length is already comparable to bulk nonlinear crystals.

In conclusion, in this letter, we propose and analyze a silica-based optical fiber with large and thermodynamically stable second order nonlinearity. Furthermore, we demonstrate that instead of being a hindrance, the cylindrical symmetry of the nonlinear fiber can naturally lead to the generation of polarization entangled photon pairs. Consequently, the proposed nonlinear fiber can significantly advance the development of nonlinear fiber optics and quantum information technology.

<sup>1</sup>Robert W. Boyd, *Nonlinear Optics*, 2nd ed. (Academic, San Diego, 2003), p. 42.

<sup>2</sup>Amnon Yariv and Pochi Yeh, *Photonics: Optical Electronics in Modern Communications*, 6th ed. (Oxford University Press, New York, 2007), pp. 361 and 362.

<sup>3</sup>Y. Xu, R. K. Lee, and A. Yariv, *J. Opt. Soc. Am. B* **17**, 387 (2000).

<sup>4</sup>T. C. Ralph, *Rep. Prog. Phys.* **69**, 853 (2006).

<sup>5</sup>P. G. Kwiat, K. Mattle, H. Weinfurter, and A. Zeilinger, *Phys. Rev. Lett.* **75**, 4337 (1995).

<sup>6</sup>U. Osterberg and W. Margulis, *Opt. Lett.* **11**, 516 (1986).

<sup>7</sup>R. A. Myers, N. Mukherjee, and S. R. Brueck, *Opt. Lett.* **16**, 1732 (1991).

<sup>8</sup>T. Fujiwara, M. Takahashi, and A. J. Ikushima, *Appl. Phys. Lett.* **71**, 1032 (1997).

<sup>9</sup>A. L. Moura, M. T. de Araujo, M. V. D. Vermelho, and J. S. Aitchison, *J. Appl. Phys.* **100**, 033509 (2006).

<sup>10</sup>G. Decher, *Science* **277**, 1232 (1997).

<sup>11</sup>W. Liang, Y. Huang, Y. Xu, R. K. Lee, and A. Yariv, *Appl. Phys. Lett.* **86**, 151122 (2005).

<sup>12</sup>J. R. Heflin, M. T. Guzy, P. J. Neyman, K. J. Gaskins, C. Brands, Z. Wang, H. W. Gibson, R. M. Davis, and K. E. Van Cott, *Langmuir* **22**, 5723 (2006).

<sup>13</sup>M. Jager, G. I. Stegeman, M. C. Flipse, M. Diemeer, and G. Mohlmann, *Appl. Phys. Lett.* **69**, 4139 (1996).